

Interfacial free energy and medium range order: Proof of an inverse of Frank's hypothesisGeun Woo Lee,^{1,2,*} Yong Chan Cho,¹ Byeongchan Lee,^{3,†} and Kenneth F. Kelton⁴¹*Division of Convergence Technology, Korea Research Institute of Standards and Science, 305-340, Republic of Korea*²*Department of Nano Science, Korea University of Science and Technology, Daejeon, 305-333, Republic of Korea*³*Department of Mechanical Engineering, Kyung Hee University, Yongin, Gyeonggi 17104, Republic of Korea*⁴*Department of Physics, Washington University, St. Louis, Missouri 63130, USA*

(Received 15 September 2016; revised manuscript received 26 December 2016; published 13 February 2017)

We study the relation of crystal-liquid interfacial free energy and medium range order in the quasicrystal-forming $\text{Ti}_{37}\text{Zr}_{42}\text{Ni}_{21}$ liquid from undercooling experiment and *ab initio* molecular dynamics (MD) simulation. Adding a small amount of Ag to the liquid significantly reduces the degree of undercooling, which is suggestive of small interfacial free energy, and thus very similar atomic configuration between the liquid and the icosahedral quasicrystal phases. Using *ab initio* MD study, we find that Ag atoms predominantly form a bond with Zr atoms in the short range and, further, Ag-Zr pairs are extended in the liquid, as a medium range order which is identical to the global structural feature reported recently [Liu *et al.*, *Phys. Rev. Lett.* **105**, 155501 (2010)]. This result may expect extremely small undercooling if the icosahedral medium range order exists in a liquid forming an icosahedral quasicrystal, which implies the ambiguity of clear distinction of heterogeneous and homogeneous nucleation.

DOI: [10.1103/PhysRevB.95.054202](https://doi.org/10.1103/PhysRevB.95.054202)**I. INTRODUCTION**

Icosahedral short-range order (ISRO) and crystal-liquid interfacial free energy have been considered as key factors to understand deep supercooling phenomena and glass forming ability of liquid metals and alloys. The lower energy and the higher packing density of ISRO clusters than those of close-packed crystal order clusters (e.g., bcc, fcc, and hcp) could explain the stability of the supercooled liquid [1]. Moreover, the noncrystallographic cluster ISRO is not compatible with the periodicity of crystallographic clusters. Thus the structural difference between ISRO and close-packed crystal orders can produce the large difference of configurational entropy, resulting in high interfacial energy and high nucleation barrier, when crystal nuclei form [2,3].

Experimental vindication for the above hypothesis was provided by the combination of levitation and diffraction techniques; the presence of ISRO was directly observed for elements and alloys in x-ray [4–7] and neutron diffraction studies [8,9]. Moreover, it was demonstrated that the amount of undercooling and the crystal-liquid interfacial free energy (or nucleation barrier) depended on the similarity of the ISRO in liquids and local orders of the crystals; for simple crystalline phases of elemental transition metal and alloy liquids [4,5,10,11], the interfacial energy [σ (J/m²)] per fusion enthalpy (ΔH_f) [i.e., Turnbull coefficient α ($= \sigma/\Delta H_f$)] and undercooling ($\Delta T/T_m$) were about 0.39 to 0.61, and about 0.16 to 0.25, respectively, which show the highest values compared with other crystal phases. For complex polytetrahedral phases [4,5,12], the corresponding values were about 0.37 to 0.43, and about 0.12 to 0.15, respectively. For quasicrystalline phases [4,5,12], the lowest α was shown to be about 0.32 to 0.34, and the undercooling about 0.09 to 0.11, respectively: quasicrystalline phases in general show the lowest nucleation barrier of all.

The above results imply that the SRO of liquids may act as a template, i.e., a type of “heterogeneous” nucleation site, if the SRO of liquids is the same as that of the competing crystal phases, and thus lowers the crystal-liquid interfacial energy [4]. This means that the homogeneity of the disordered state can be locally broken in time and space. The effect of the structural heterogeneity may be accelerated by an extended local order or a medium range order. For instance, a supercooled colloidal liquid can stay in a transient state of medium-range structural ordering, which can stimulate crystallization [13]. This means that the supercooled liquid is not in a purely homogeneous state; the medium range order (MRO) could reduce the interfacial free energy (thus nucleation barrier) if the MRO of liquid is similar to that of a crystal.

In the case of bulk metallic glasses (BMG), the icosahedral medium range order (IMRO) (or extended ISRO) in liquids often plays a significant role in improving glass forming ability (GFA) by increasing the nucleation barrier (or interfacial free energy) for crystal formation [14–18]. In the case of quasicrystals, on the other hand, a quasicrystal growth is facilitated by structurally persistent atoms that are kinetically trapped in icosahedral clusters nearby the quasicrystal nucleus [19,20], which reflects the existence of a structural correlation longer than SRO.

Although the structural heterogeneity of MRO affecting the formation of glasses and crystals has been extensively studied [13–28], its direct relationship with the interfacial free energy is still elusive. In addition, IMRO does not always appear as a pre-peak in total structure factor of liquids and glasses, caused by chemical/topological ordering, when the constituents of the liquids and glasses are miscible or too many. Moreover, impurities (e.g., container wall) in liquids become obstacles to study the crystal-liquid interfacial free energy. This prevents a clear understanding of the relation of the IMRO and interfacial free energy, which attributes to the GFA and mechanical properties of BMG [14–16], and to the quality of quasicrystals [29].

In the present work, we study the relation of IMRO and nucleation barrier (or interfacial free energy) of Ti-Zr-Ni

*gwlee@kriss.re.kr

†airbc@khu.ac.kr

icosahedral quasicrystals using electrostatic levitation (ESL) and *ab initio* MD calculations, providing undercooling experiment under containerless environment and detailed structural information, respectively. Here, we choose $\text{Ti}_{37}\text{Zr}_{42}\text{Ni}_{21}$ alloy forming icosahedral quasicrystals (i-phase) congruently [5,30,31], and add a small amount of Ag to the alloy since the melts have ISRO and the i-phase with Ag shows longer crystal coherence length [4,7,29]. In this work, we find that Ag addition to $\text{Ti}_{37}\text{Zr}_{42}\text{Ni}_{21}$ liquid gives a smaller undercooling and a smaller crystal-liquid interfacial free energy than the liquid prepared without Ag. We also provide the structural evidence for IMRO in the $(\text{Ti}_{37}\text{Zr}_{42}\text{Ni}_{21})_{96}\text{Ag}_4$ liquid using *ab initio* MD simulation. Accordingly, we conclude that IMRO formed by Ag addition lowers the interfacial free energy and the undercoolability of the Ti-Zr-Ni liquid. These results are consistent again with Frank's hypothesis, but inverse aspect; the nucleation barrier becomes smaller when the structure of the liquid and the competing crystal phases are similar.

II. EXPERIMENT AND SIMULATION

Ingots (0.5 g) of $(\text{Ti}_{37}\text{Zr}_{42}\text{Ni}_{21})_{(100-x)}\text{Ag}_x(x=0,2,4,8)$ (Ti purity, 99.995%; Zr purity, 99.95%; Ni purity, 99.995%; Ag purity 99.99%) were prepared by arc melting on a water-cooled Cu hearth under high-purity Ar gas (purity, 99.995%). The ingots were flipped and remelted at least five times to achieve sample homogeneity. The ingots were cracked and remelted to obtain smaller ingots, less than 0.05 g. Mass losses after melting were 0.2%. Structural information for the i-phase was obtained by x-ray diffraction (XRD) using Cu $K\alpha$ radiation. Undercooling studies were made on samples 2.3–2.5 mm diameter that were levitated using electrostatic levitation. Detailed experimental procedure and device are reviewed elsewhere [32].

The structural properties were calculated from molecular dynamics using the Vienna *ab initio* software package (VASP) with the projector augmented-wave method [33,34] and the generalized gradient approximation [35]. The energy cutoff of 19.81 Ry at the Γ point was used to obtain the structural properties from the average of 1 ps with a 1 fs time step. Both $\text{Ti}_{37}\text{Zr}_{42}\text{Ni}_{21}$ and $(\text{Ti}_{37}\text{Zr}_{42}\text{Ni}_{21})_{96}\text{Ag}_4$ systems were simulated with the closest possible cell sizes; the exact compositions used are given in Table I. Each system is equilibrated at 877 °C for at least 20 ps and then supercooled to 757 °C and held for 12 ps or longer.

III. RESULTS AND DISCUSSION

Figure 1 shows time-temperature curves of $\text{Ti}_{37}\text{Zr}_{42}\text{Ni}_{21}$ liquid. A double step-recalescence is found in the first, fourth,

TABLE I. Compositions of simulation cells.

System	Number of atoms (fraction)				Total
	Ti	Zr	Ni	Ag	
$\text{Ti}_{37}\text{Zr}_{42}\text{Ni}_{21}$	155 (0.370)	176 (0.420)	88 (0.210)		419 (1.000)
$(\text{Ti}_{37}\text{Zr}_{42}\text{Ni}_{21})_{96}\text{Ag}_4$	148 (0.355)	168 (0.403)	84 (0.201)	17 (0.041)	417 (1.000)

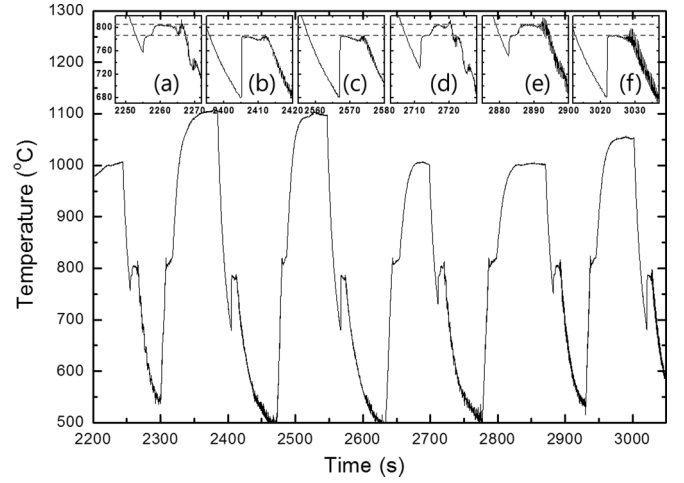


FIG. 1. Temperature-time curves for a $\text{Ti}_{37}\text{Zr}_{42}\text{Ni}_{21}$ liquid. The inset figures show the recalescence behaviors of each cycle. The spiked features in the temperature at the end of the plateaus and after the plateaus are caused by surface roughness due to crystallization. Case (I) is of (a), (d), and (e), and case II is of (b), (c), and (f).

and fifth cycles [see Figs. 1(a), 1(d), and 1(e), case (I)]. This is a typical feature indicating the formation of the i-phase from the supercooled liquid as reported in previous works [4,5,29,31]. The first recalescence (plateau temperature ~ 785 °C) is due to the formation of the icosahedral quasicrystal phase (i-phase), and the second recalescence (plateau temperature ~ 805 °C) is the result of the decomposition of the i-phase into a poly-tetrahedral crystalline phase (C14 Laves phase) [4,5,29,31]. However, the liquid often deeply supercools and shows just one recalescence at approximately 680 °C [Figs. 1(b), 1(c), and 1(f), case (II)]. The plateau temperature of this single recalescence is about 785 °C, which is consistent with the melting temperature of i-phase. These recalescence behaviors occur statistically, resulting from a sampling of the energy landscape of the supercooled liquid.

The classical homogeneous nucleation theory (CNT) can provide a more detailed understanding for the above phenomena. In general, at a given small undercooling, large critical size of nuclei is needed to initiate crystallization, since the critical radius of nuclei is given by $r^* = 2\sigma/\Delta G_v^{l-s} = 2\sigma T_m/(\Delta H_f \Delta T)$, where σ , ΔG_v^{l-s} , T_m , ΔH_f , and ΔT are interfacial free energy, driving volume Gibbs energy, melting temperature, fusion enthalpy, and undercooling, respectively. In addition, nucleation barrier at the small undercooling should be large, since the barrier is inversely proportional to supercooling, i.e., $\Delta G^* = (16\pi/3)\sigma^3/(\Delta G_v^{l-s})^2 = (16\pi/3)\sigma^3 [T_m/(\Delta H_f \Delta T)]^2$. Therefore, small undercooling is less likely to form stable nuclei, resulting in no significant crystallization. Nevertheless, the fact, the formation of the i-phase in case (I), suggests that the interfacial energy between the liquid and the quasicrystal should be small enough to compensate the small driving force for nucleation.

Using CNT, we study the critical nucleus in details as we did in previous studies [4,5,11]. The estimated critical nucleus size is about 5.10 nm for the smallest supercooling (757 °C) [case (I)], and is about 3.44 nm for the deep supercooling [case (II) in Figs. 1(b), 1(c), and 1(f), and see Table II]. This

TABLE II. Reduced undercooling, interfacial free energy, Turnbull coefficient, nucleation barrier, critical radius of $\text{Ti}_{37}\text{Zr}_{42}\text{Ni}_{21}$ and $(\text{Ti}_{37}\text{Zr}_{42}\text{Ni}_{21})_{96}\text{Ag}_4$ liquids, and the coherence length of the as cast i-phase. Samples I and II correspond to cases (I) and (II) in Fig. 1, respectively. Parentheses values are of $W^*/k_B T$ at the recalescence temperature of each case: $\Delta G_{l-s}(1) = \frac{\Delta T \Delta H_f}{T_i}$, $\Delta G_{l-s}(2) = \frac{\Delta T \Delta H_f}{T_m} \frac{2T}{T_i + T}$, $\Delta G_{l-s}(3) = \frac{\Delta T \Delta H_f}{T_m} - \gamma \Delta S_f [\Delta T - T \ln(\frac{T}{T_i})]$.

Samples and used parameters ($T_m, \rho, C_p, \Delta H_f$)	$\Delta T/T_m$	Interfacial energy (σ) (± 0.0002)			$\alpha(=\sigma/\Delta H_f)$	$W^*/k_B T$ [at T_r of $(\text{Ti}_{37}\text{Zr}_{42}\text{Ni}_{21})_{96}\text{Ag}_4$]	$r^*(l)$ (nm)	Coherence length (nm) on as cast i-phase
		$\Delta G_{l-s}(1)$	$\Delta G_{l-s}(2)$	$\Delta G_{l-s}(3)$				
(I) $\text{Ti}_{37}\text{Zr}_{42}\text{Ni}_{21}$ ($T_m = 1060$ K, $\rho = 5.95$ g/cm ³ , $C_p = 44.24$ J/mol K, $\Delta H_f = 8.1$ kJ/mol)	0.03	0.030	0.024	0.024	0.160	74.34 (61.27)	2.549	25
(II) $\text{Ti}_{37}\text{Zr}_{42}\text{Ni}_{21}$ ($T_m = 1060$ K, $\rho = 5.95$ g/cm ³ , $C_p = 44.24$ J/mol K, $\Delta H_f = 8.1$ kJ/mol)	0.1	0.061	0.049	0.050	0.324	665.17 (58.49)	1.735	
(III) $(\text{Ti}_{37}\text{Zr}_{42}\text{Ni}_{21})_{96}\text{Ag}_4$ ($T_m = 1060$ K, $\rho = 5.98$ g/cm ³ , $C_p = 44.24$ J/mol K, $\Delta H_f = 7.93$ kJ/mol)	0.029	0.027	0.022	0.022	0.146	58.84 (58.84)	2.736	43

is much larger than the size, 1.046 nm, of the Bergman cluster composed of 45 atoms. (Note that Ti-Zr-Ni quasicrystals are of a Bergman type [36], where Ni is the center atom, the first shell is occupied by 12 Ti atoms, and the second shell is occupied by Zr on the 20 faces of Ti atoms in the first shell, and the third shell is composed of Ni atoms at the vertexes of the 12 Ti atoms.) The critical nuclei size for elemental transition metal liquids is usually smaller than ~ 3.4 nm at hypercooling temperatures [10,11]. For a Zr liquid, the critical nuclei size is ~ 3.2 nm at the hypercooling temperature 1481 °C [11]. The nuclei with size 5.1 nm in case (I) include 3000 atoms more than in the case of Zr. It is hard to imagine the formation of such large critical size of nuclei by long range atomic diffusion of each element, since the complicated structural aperiodicity and large size of icosahedral quasicrystal nuclei require long distance diffusion of the elements. Therefore, it is rational to assume that the crystal nucleation occurs by just density fluctuation of medium range order (MRO), if the MRO exists already in the liquid. Moreover, the crystal-supercooled liquid interfacial free energies (σ) for the i-phase estimated by CNT are small, i.e., 0.030 (J/m²) and 0.061 (J/m²) for cases (I) and (II) respectively (Table II). The small interfacial energy reflects the structural similarity between the liquid and i-phase since the interfacial energy results from a configurational entropy difference between liquid and crystal [2,3]. Similarly, Al-based alloys showed small interfacial energy 0.091–0.094 (J/m²) for the liquid/icosahedral quasicrystal phase, but larger values 0.153–0.182 (J/m²) for the liquid/crystal phases [12]. Consequently, the larger nuclei size than the size of 45-atoms Bergman cluster and small interfacial energies for case (I) strongly manifest the existence of an extended local order, i.e., a medium range order, in the supercooled $\text{Ti}_{37}\text{Zr}_{42}\text{Ni}_{21}$ liquid.

The aforementioned structure-energy relationship can be even more evident if ISRO is extended to a longer range in liquids that form icosahedral quasicrystals. We have found that a small addition of Ag substantially changes the formation and stability of Ti-Zr-Ni quasicrystals in our previous study [29];

the average coherence length of the as-cast i-phase increases from 25 nm to 31 nm by adding 2 at. % Ag, and further to 43 ± 4 nm with the addition of 4 at. % Ag. The addition of 8 at. % Ag destabilizes the formation of the i-phase and enhances the formation of the C14 Laves phase [29]. Because it has the longest coherence length, we selected $(\text{Ti}_{37}\text{Zr}_{42}\text{Ni}_{21})_{96}\text{Ag}_4$ to study the relation of interfacial free energy and icosahedral medium range order (IMRO) in the liquid.

Figure 2 shows the temperature-time curves for the $(\text{Ti}_{37}\text{Zr}_{42}\text{Ni}_{21})_{96}\text{Ag}_4$ liquid. Unlike case (I) of $\text{Ti}_{37}\text{Zr}_{42}\text{Ni}_{21}$ [Figs. 1(a), 1(d), and 1(e)], $(\text{Ti}_{37}\text{Zr}_{42}\text{Ni}_{21})_{96}\text{Ag}_4$ always shows a single recalescence even with shallow undercooling (757 °C). Note that the $\text{Ti}_{37}\text{Zr}_{42}\text{Ni}_{21}$ liquid shows also small undercooling in Figs. 1(a), 1(d), and 1(e), but it shows double recalescence. The single recalescence indicates the formation of the i-phase only with a shallow undercooling. Since the Laves phase is stable at this temperature [4,5,29,31], staying longer at the melting temperature of the i-phase should increase the possibility to form the Laves phase, which does not happen in Fig. 2(b). Therefore, the addition of Ag stabilizes the i-phase relative to the C14 Laves phase. This is consistent with annealing experiments [29], showing that the i-phase with Ag additions still existed at 600 °C after 5 days, but the i-phase with no Ag addition transformed into Laves phase under the same conditions.

We again applied the classical nucleation theory (CNT) to estimate the crystal-liquid interfacial free energy, the nucleation barrier, and the critical size for the i-phase nucleation. The interface energy of $(\text{Ti}_{37}\text{Zr}_{42}\text{Ni}_{21})_{96}\text{Ag}_4$ is less than half of $\text{Ti}_{37}\text{Zr}_{42}\text{Ni}_{21}$ with no Ag (see sample III in Table II). Also Turnbull coefficient (α) reflecting the structural similarity of liquid and crystal at interface is 0.146 for $(\text{Ti}_{37}\text{Zr}_{42}\text{Ni}_{21})_{96}\text{Ag}_4$, significantly smaller than 0.32 for $\text{Ti}_{37}\text{Zr}_{42}\text{Ni}_{21}$.

Therefore, the nucleation barrier of i-phase $(\text{Ti}_{37}\text{Zr}_{42}\text{Ni}_{21})_{96}\text{Ag}_4$ is also lower than that of $\text{Ti}_{37}\text{Zr}_{42}\text{Ni}_{21}$ [case (I)] at the same temperature [see Fig. 3(a)]. The critical radius of nuclei is about 5.47 nm for $(\text{Ti}_{37}\text{Zr}_{42}\text{Ni}_{21})_{96}\text{Ag}_4$, which is larger than 3.44 nm for $\text{Ti}_{37}\text{Zr}_{42}\text{Ni}_{21}$ [Fig. 3(b) and

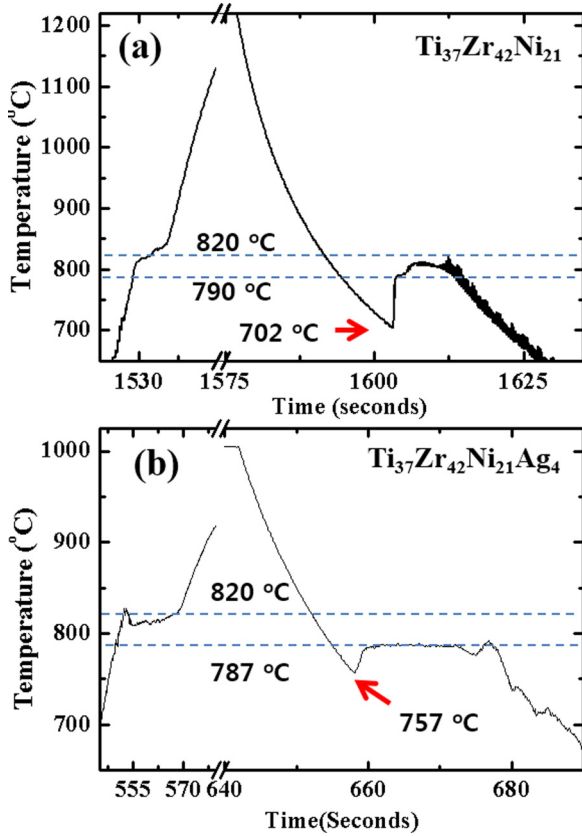


FIG. 2. Temperature-time curves of $\text{Ti}_{37}\text{Zr}_{42}\text{Ni}_{21}$ (a) and $(\text{Ti}_{37}\text{Zr}_{42}\text{Ni}_{21})_{96}\text{Ag}_4$ (b). Melting temperature of i-phase is indicated at 790 °C and 787 °C in (a) and (b), respectively. The melting temperature for Laves phase is 820 °C. Panel (a) shows only the recalescence behavior for each sample.

Table II]. On considering multicomponent and elaborated aperiodicity of the i-phase, a large size of clusters should be fluctuated to form such a large critical size of i-phase nuclei in liquid. In other words, an extended local ordering like IMRO cluster should exist in the liquid.

To scrutinize the IMRO, we have performed *ab initio* molecular dynamic simulations. The total pair distribution

functions, $g(r)$, show no significant difference between the two supercooled liquids with or without Ag, except for slightly sharper peaks on $(\text{Ti}_{37}\text{Zr}_{42}\text{Ni}_{21})_{96}\text{Ag}_4$ [Fig. 4(a)]. The alloying of Ag barely changes the partial pair distribution functions (PDF) among Ti, Zr, and Ni [Figs. 4(b) and 4(c)], only slightly decreasing the intensity of these partials due to the reduced amount of Ti-Zr-Ni.

However, a critical change is found around Ag atoms as shown in Fig. 4(d). Ag atoms preferably attract Zr atoms in the nearest neighbor shell, suggesting a change in ordering, whether it is topological or chemical. Ag naturally prefers Zr atoms due to high negative heat of mixing [e.g., Ag-Ti (−2 kJ/mol) and Ag-Zr (−43 kJ/mol)] [37]. Moreover, the atomic size ratio of Ag to Zr, $0.90 [= \text{Ag}(2.88 \text{ \AA})/\text{Zr}(3.2 \text{ \AA})]$, which is closer to the ideal ISRO value of 0.902 than other constituents [23,38], facilitates the formation of Ag-Zr pair-abundant icosahedral clusters resulting in a higher packing density and lower energy. To obtain topological information of the local orders, we carried out the Honeycutt-Anderson (HA) analysis (Fig. 5). The HA analysis shows the large number of (1431), (1541), and (1551) pairs for both liquids which are the fragments of ISRO and indicate prevailing ISRO in the liquid. Those observations suggest that the addition of Ag atoms increased the number of ISRO clusters with dominantly pairing Zr atoms in the liquid. Moreover, the decreasing (1441) and (1661) pairs with Ag indicates that bcc and hcp crystalline order are suppressed. This is consistent with the observation of an absence of the Laves phase (hcp) in $(\text{Ti}_{37}\text{Zr}_{42}\text{Ni}_{21})_{96}\text{Ag}_4$ in Fig 2.

Although we see a significant fraction of ISRO from the PDF and the HA analyses based on the nearest atomic configuration, information about IMRO is still unclear from this analysis. In many cases, the MRO has been often observed as a prepeak in the total structure factor, indicating chemical/topological ordering at low q . However, such a prepeak was not clearly presented in the total structure factor of Ti-Zr-Ni alloy liquids in our previous study [7,39] as well as in many metallic glasses.

Nevertheless, the information of MRO may still be present in the $g(r)$, but may turn up from a different viewpoint of $g(r)$. Liu and co-workers have found a global structure feature of the MRO from the PDF [23]; the ratio of peak positions to the first peak in $g(r)$ falls in to $1.73 (= \sqrt{3})$, $2.00 (= \sqrt{4})$, $2.64 (\sqrt{7})$,

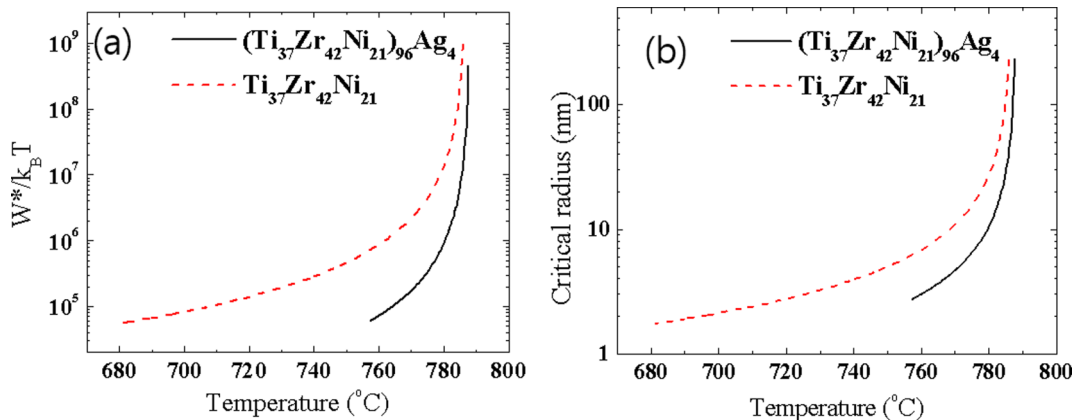


FIG. 3. Calculated nucleation barriers and critical radii for Ti-Zr-Ni quasicrystals with and without Ag. Assuming $\Delta G_{I-s}(l) = \frac{\Delta T \Delta H_f}{T_i}$.

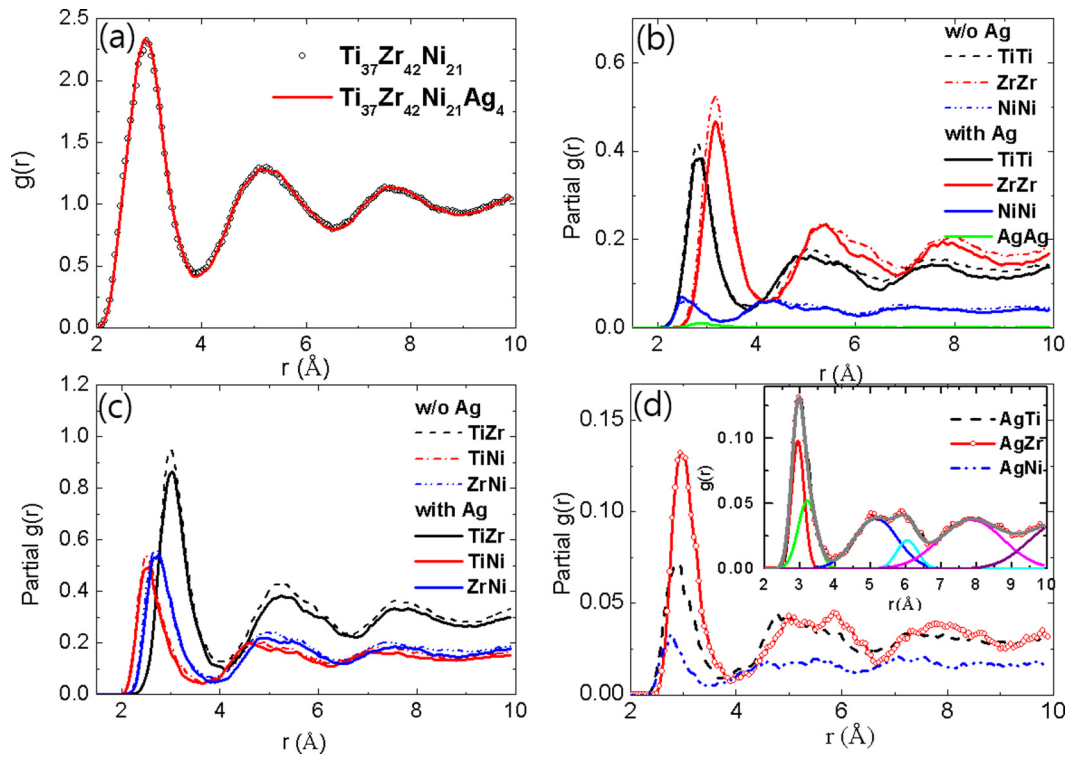


FIG. 4. Pair distribution function, $g(r)$, of supercooled $\text{Ti}_{37}\text{Zr}_{42}\text{Ni}_{21}$ and $(\text{Ti}_{37}\text{Zr}_{42}\text{Ni}_{21})_{96}\text{Ag}_4$ liquids at 757 °C. (a) Total $g(r)$. (b) Partial $g(r)$'s for the same atomic pairs. (c) Partial $g(r)$'s for different atomic pairs. (d) Partial $g(r)$'s with transition metal–Ag pairs. Inset in (d) shows the fitting curve for $g(r)$ of Ag-Zr pair with six Gaussian curves (the gray color is of total fitting curve).

and $3.46(=\sqrt{12})$ for all 64 metallic glasses. This finding suggests that the SRO and MRO are described by spherical-periodic order (SPO) and local translational symmetry (LTS) [24]. We tested the global structural feature as shown in Table III. Atomic pairs between Ti, Zr, and Ni give almost no change of the positions with and without Ag addition. But

the normalized peak positions of Ag pairs with Ti and Zr agree with the global feature discussed by Liu *et al.* [24]. In particular, Ag-Zr pair shows good agreement with the global values indicating the MRO.

The peak positions of $g(r)$ in the liquid are predicted by spherical periodic order (SPO), which is given by $R_n = (n + 1/4)\lambda_F$, where the Friedel wavelength $\lambda_F = 2\pi/2k_F$, and Fermi-sphere diameter $2k_F$ [25]. The theoretically expected values are $R_2/R_1 = 1.8$, $R_3/R_1 = 2.6$, and $R_4/R_1 = 3.4$, respectively. Although those values are quite close to the global peak positions, the ratio of 2 is missing. Liu and co-workers have argued that the missing value, 2, was the result of an additional ordering mechanism, i.e., local translational symmetry (LTS) during the glass transition, which originated from long-lived medium range crystalline order (MRCO) [24]. In the present study, icosahedral clusters may be the MRCO, although we are treating liquid, but not glass. A recent study [26] supports this picture in that the MRO formed by two icosahedral clusters sharing a vertex atom provides the missing value of 2. That is, the medium range order of the 19-atoms icosahedron showed the normalized peak positions $R_2/R_1 = 1.701$, $R_3/R_1 = 2$, and $R_4/R_1 = 2.605$. If we consider multiple components with different atomic sizes in the Ti-Zr-Ni-Ag alloy, the values are quite similar to the global features from the PDF. Consequently, the normalized peak positions of Ag-Zr pair indicate the existence of IMRO in the liquid. It should be noted that $\text{Ti}_{37}\text{Zr}_{42}\text{Ni}_{21}$ liquid does not show the global structural feature of peak positions in $g(r)$, which may give the deeper undercooling than $(\text{Ti}_{37}\text{Zr}_{42}\text{Ni}_{21})_{96}\text{Ag}_4$ liquid.

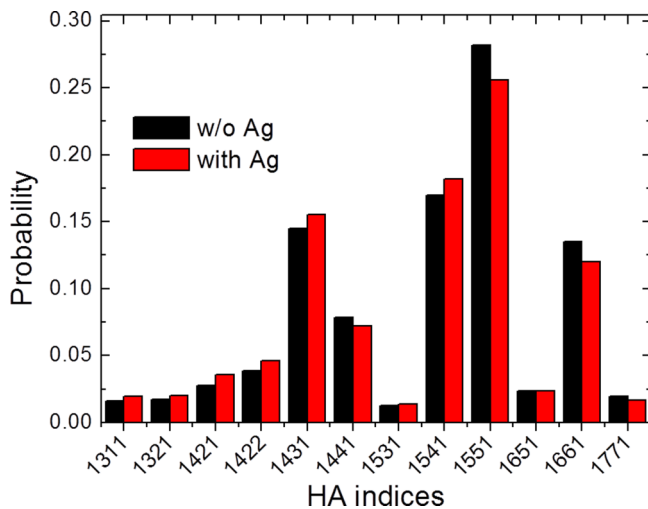


FIG. 5. Analysis of the $\text{Ti}_{37}\text{Zr}_{42}\text{Ni}_{21}$ and $(\text{Ti}_{37}\text{Zr}_{42}\text{Ni}_{21})_{96}\text{Ag}_4$ obtained from MD simulations using the Honeycutt-Anderson (HA) method with a cutoff, $r_{\text{cutoff}} 3.9 \text{ \AA}$, which is the first minimum in $g(r)$ in Fig. 4(a).

TABLE III. Peak positions directly obtained from the partial $g(r)$ of $(\text{Ti}_{37}\text{Zr}_{42}\text{Ni}_{21})_{96}\text{Ag}_4$ in Fig. 4(d) by six Gaussian curve fittings. $R_1(\text{av})$ [i.e., the first peak of $g(r)$], as done in Ref. [24]. The values in parentheses are of the peak positions of partial $g(r)_{\text{Ti}_{37}\text{Zr}_{42}\text{Ni}_{21}}$.

Type	$R_1(\text{av})$	R_2	R_3	R_4	R_5	$R_2/R_1(\text{av})$ 1.73^a	$R_3/R_1(\text{av})$ 2.00^a	$R_4/R_1(\text{av})$ 2.64^a	$R_5/R_1(\text{av})$ 3.46^a
Ti-Ag	2.93	5.00	5.93	7.54	10.33	1.71	2.02	2.57	3.53
Zr-Ag	2.97	5.12	6.03	7.84	10.30	1.72	2.03	2.64	3.48
Ti-Ni	2.52	4.67	5.59	7.14	9.89	1.85	2.22	2.83	3.93
	(2.52)	(4.73)	(5.67)	(7.2)	(9.90)	(1.88)	(2.25)	(2.86)	(3.93)
Zr-Ni	2.72	4.94	5.82	7.47	10.05	1.82	2.14	2.75	3.67
	(2.71)	(4.98)	(5.2)	(7.38)	(10.17)	(1.84)	(1.92)	(2.72)	(3.75)
Ti-Zr	3.01	5.24	6.18	7.56	10.19	1.74	2.05	2.51	3.39
	(3.00)	(5.23)	(6.17)	(7.56)	(10.09)	(1.74)	(2.06)	(2.52)	(3.36)

^adenotes the global values in Ref. [24].

IV. CONCLUSIONS

In summary, we have studied the relation of interfacial free energy and medium range order in liquids that form an icosahedral quasicrystal. It is found that a small amount of Ag added to $\text{Ti}_{37}\text{Zr}_{42}\text{Ni}_{21}$ facilitates the formation ISRO and IMRO in the liquid from the undercooling experiment and the PDF study using ESL and *ab initio* MD simulation. Using CNT, we estimated larger critical size 5.4 nm of the nuclei and smaller liquid-crystal interfacial free energy in $(\text{Ti}_{37}\text{Zr}_{42}\text{Ni}_{21})_{96}\text{Ag}_4$ than in $\text{Ti}_{37}\text{Zr}_{42}\text{Ni}_{21}$. Since the nucleation is stochastic and fluctuation phenomenon, the observation of the large critical size of nuclei and small interfacial free energy in the alloy liquid with multicomponent strongly manifest the extended ISRO or icosahedral medium-range order. From *ab initio* MD simulation study, we have found the evidence of IMRO reflecting the global structural feature in $(\text{Ti}_{37}\text{Zr}_{42}\text{Ni}_{21})_{96}\text{Ag}_4$ liquid, but absent in $\text{Ti}_{37}\text{Zr}_{42}\text{Ni}_{21}$ liquid. Therefore, the small undercooling and interfacial free energy underlies the existence of IMRO. Here, it is worthwhile to mention an extreme case; the present work

can be extended in search of liquids with extremely small undercooling where the IMRO percolates throughout the liquid or becomes sufficiently dominant in the liquid with high population, even above liquidus temperature. We may expect extremely small undercooling with some stable quasicrystals with chemical or topological SRO having a well-defined stoichiometric composition of the i-phase. This is the inverse of deep undercooling, corresponding to an inverse Frank's hypothesis.

ACKNOWLEDGMENTS

This research was supported by the Converging Research Center Program through the Ministry of Science, ICT and Future Planning, Korea (Grants No. NRF-2014M3C1A8048818 and No. NRF-2014M1A7A1A01030128), and by the Mid-Career Researcher Support Program (Grant No. NRF-2014R1A2A2A09052374). K.F.K. gratefully acknowledges support from the National Science Foundation under Grant No. DMR-15-06553.

- [1] F. C. Frank, *Proc. R. Soc.* **215A**, 43 (1952).
- [2] F. Spaepen and R. Meyer, *Scr. Metall.* **10**, 257 (1976).
- [3] F. Spaepen, *Acta Metall.* **23**, 729 (1975).
- [4] K. F. Kelton, G. W. Lee, A. K. Gangopadhyay, R. W. Hyers, T. J. Rathz, J. R. Rogers, M. B. Robinson, and D. S. Robinson, *Phys. Rev. Lett.* **90**, 195504 (2003).
- [5] G. W. Lee, A. K. Gangopadhyay, T. K. Croat, T. J. Rathz, R. W. Hyers, J. R. Rogers, and K. F. Kelton, *Phys. Rev. B* **72**, 174107 (2005).
- [6] G. W. Lee, A. K. Gangopadhyay, K. F. Kelton, R. W. Hyers, T. J. Rathz, J. R. Rogers, and D. S. Robinson, *Phys. Rev. Lett.* **93**, 037802 (2004).
- [7] G. W. Lee, A. K. Gangopadhyay, R. W. Hyers, T. J. Rathz, J. R. Rogers, D. S. Robinson, A. I. Goldman, and K. F. Kelton, *Phys. Rev. B* **77**, 184102 (2008).
- [8] T. Schenk, D. Holland-Moritz, V. Simonet, R. Bellissent, and D. M. Herlach, *Phys. Rev. Lett.* **89**, 075507 (2002).
- [9] T. Schenk, V. Simonet, D. Holland-Moritz, R. Bellissent, T. Hansen, P. Convert, and D. M. Herlach, *Europhys. Lett.* **65**, 34 (2004).
- [10] B. Vinet, L. Magnusson, H. Fredriksson, and P. J. Desré, *J. Colloid. Interface Sci.* **255**, 363 (2002).
- [11] D.-H. Kang, S. Jeon, H. Yoo, T. Ishikawa, J. T. Okada, P.-F. Paradis, and G. W. Lee, *Cryst. Growth Design* **14**, 1103 (2014).
- [12] D. Holland-Moritz, J. Schroers, D. M. Herlach, B. Grushko, and K. Urban, *Acta Mater.* **46**, 1601 (1998).
- [13] T. Kawasaki and H. Tanaka, *Proc. Natl. Acad. Sci. USA* **107**, 14036 (2010).
- [14] Y. Shi and M. L. Falk, *Phys. Rev. Lett.* **95**, 095502 (2005).
- [15] R. Soklaski, Z. Nussinov, Z. Markow, K. F. Kelton, and L. Yang, *Phys. Rev. B* **87**, 184203 (2013).
- [16] M. Lee, C.-M. Lee, K.-R. Lee, E. Ma, and J.-C. Lee, *Acta Mater.* **59**, 159 (2011).
- [17] X. W. Fang, C. Z. Wang, S. G. Hao, M. J. Kramer, Y. X. Yao, M. I. Mendeleev, Z. J. Ding, R. E. Napolitano, and K. M. Ho, *Sci. Rep.* **1**, 194 (2011).
- [18] D.-H. Kang, H. Zhang, H. Yoo, H. H. Lee, G. W. Lee, H. Lou, X. Wang, Q. Cao, D. Zhang, and J. Jiang, *Sci. Rep.* **4**, 5167 (2014).

- [19] P. J. Steinhardt, *Nature (London)* **452**, 43 (2008).
- [20] A. S. Keys and S. C. Glotzer, *Phys. Rev. Lett.* **99**, 235503 (2007).
- [21] N. A. Mauro and K. F. Kelton, *J. Non-Cryst. Solids* **358**, 3057 (2012).
- [22] N. A. Mauro, V. Wessels, J. C. Bendert, S. Klein, A. K. Gangopadhyay, M. J. Kramer, S. G. Hao, G. E. Rustan, A. Kreyssig, A. I. Goldman, and K. F. Kelton, *Phys. Rev. B* **83**, 184109 (2011).
- [23] D. B. Miracle, *Nat. Mater.* **3**, 697 (2004); *J. Non-Cryst. Solids* **342**, 89 (2004).
- [24] X. J. Liu, Y. Xu, X. Hui, Z. P. Lu, F. Li, G. L. Chen, J. Lu, and C. T. Liu, *Phys. Rev. Lett.* **105**, 155501 (2010).
- [25] P. Häussler, *Phys. Rep.* **222**, 65 (1992).
- [26] Y.-C. Liang, R.-S. Liu, Y.-F. Mo, H.-R. Liu, Z.-A. Tian, Q.-Y. Zhou, H.-T. Zhang, L.-L. Zhou, Z.-Y. Hou, and P. Peng, *J. Alloy Compd.* **597**, 269 (2014).
- [27] D. Ma, A. D. Stoica, and X.-L. Wang, *Nat. Mater.* **8**, 30 (2009).
- [28] L. Zhang, Y. Wu, X. Bian, H. Li, W. Wang, and S. Wu, *J. Non-Cryst. Solids* **262**, 169 (2000).
- [29] G. W. Lee, A. K. Gangopadhyay, and K. F. Kelton, *J. Alloy Compds.* **537**, 171 (2012).
- [30] G. W. Lee, T. K. Croat, A. K. Gangopadhyay, and K. F. Kelton, *Philos. Mag. Lett.* **82**, 199 (2002).
- [31] G.W. Lee, A. K. Gangopadhyay, and K. F. Kelton, *Acta Mater.* **59**, 4964 (2011).
- [32] P.-F. Paradis, T. Ishikawa, G. W. Lee, D. Holland-Moritz, J. Brillo, W.-K. Rhim, and J. T. Okada, *Mater. Sci. Eng., R* **76**, 1 (2014).
- [33] P. E. Blöchl, *Phys. Rev. B* **50**, 17953 (1994).
- [34] G. Kresse and D. Joubert, *Phys. Rev. B* **59**, 1758 (1999).
- [35] J. P. Perdew, K. Burke, and M. Ernzerhof, *Phys. Rev. Lett.* **77**, 3865 (1996).
- [36] R. G. Hennig, K. F. Kelton, A. E. Carlsson, and C. L. Henley, *Phys. Rev. B* **67**, 134202 (2003).
- [37] F. R. de Boer *et al.*, *Cohesion in Metals: Transition Metal Alloys* (North-Holland, Amsterdam, 1988).
- [38] D. R. Nelson and F. Spaepen, in *Solid State Physics*, edited by H. Ehrenreich and D. Turnbull (Academic, Boston, 1989), Vol. 2, p. 1.
- [39] T. H. Kim, G. W. Lee, A. K. Gangopadhyay, R.W. Hyers, J. R. Rogers, A. I. Goldman, and K. F. Kelton, *J. Phys.: Condens. Matter* **19**, 455212 (2007).